SANDIA REPORT
SAND2000-0829
Unlimited Release
Printed April 2000

Final CRADA Report on the Molecular Understanding of Dissolution and Stress Corrosion in Glasses

1. Spectroscopic Characterization of Aged Aluminum Borosilicate Glass

Todd M. Alam, David P. Lang, David R. Tallant, Manuel J. Garcia, Regina L. Simpson, Bonnie B. McKenzie, and Denise N. Bencoe

Prepared by
Sandia National Laboratories
Albuquerque, New Mexico 87185 and Livermore, California 94550

Sandia is a multiprogram laboratory operated by Sandia Corporation, a Lockheed Martin Company, for the United States Department of Energy under Contract DE-AC04-94AL85000.

Sandia National Laboratories

Issued by Sandia National Laboratories, operated for the United States Department of Energy by Sandia Corporation.

SAND 2000-0829
Unlimited Release
Printed April 2000

Final CRADA Report on the Molecular Understanding of Dissolution and Stress Corrosion in Glasses.

I. Spectroscopic Characterization of Aged Aluminum Borosilicate Glass.

Todd M. Alam, and David P. Lang
Organic Materials Department

David R. Tallant, Manuel J. Garcia, Regina L. Simpson, and Bonnie B. McKenzie
Materials Characterization Department

Denise N. Bencoe
Ceramic Materials Department

Sandia National Laboratories
P.O. Box 5800
Albuquerque, New Mexico, 87185-1407

Abstract

The spectroscopic characterization of aluminum borosilicate glass, both bulk glass and glass fibers, aged under aqueous conditions is reported. The characterization includes infrared, Raman, microscopic Raman, and nuclear magnetic resonance spectroscopy along with scanning electron microscopic analysis. Differences between bulk and fibers along with identification of the molecular species observed in the aged or hydrated surface are discussed.

Acknowledgements

Sandia is a multiprogram laboratory operated by Sandia Corporation, a Lockheed martin Company, for the United States Department of Energy under Contract DE-AC04-94AL85000.

Executive Summary

This report (Part I. Spectroscopic Characterization of Aged Aluminum Borosilicate Glass) summarizes the work completed on the spectroscopic characterization of dissolution in aluminum borosilicate bulk glass and fiber glass samples. The details of the computational investigations performed in conjunction with these studies will be detailed in a separate report (Part II. Cluster Model Development). A variety of spectroscopic techniques were employed to analyze the molecular structure in the unaged and aged glass samples. These techniques include scanning electron microscopy (SEM), Raman spectroscopy, infrared (IR) spectroscopy and nuclear magnetic resonance (NMR) spectroscopy. Information from these spectroscopic studies provided details about possible cluster types to incorporate into the modeling of the dissolution process. The local confirmation of the network forming components (SiO_2, Al_2O_3 and B_2O_3) in the bulk glass and glass fibers have been analyzed. In glass samples aged under acid conditions the formation of a hydrated silica "gel layer" was observed and identified using NMR, Raman and IR spectroscopy. The microscopic Raman analysis of acid aged glass fibers demonstrated that this hydrated silica gel layer is several μm thick, and shows a gradated loss of boron due to the leaching process. The NMR results demonstrate that the silanols formed during the ion exchange process within this gel layer undergo an additional condensation reaction to produce a fully condensed silicon environment. Differences in reactivity between the trigonal and tetrahedral boron species, or changed in the aluminum coordination within the aged surface were not detected using Raman or NMR spectroscopy as originally proposed.

Contents

Figures

Nomenclature

IR	infrared
SEM	scanning electron microscope
DTA	differential thermal analysis
NMR	nuclear magnetic resonance
MAS	magic angle spinning
3Q	triple quantum

1. Characterization of Unaged Aluminum Borosilicate Glass

1.1 Background

In the original CRADA proposal, spectroscopic characterization of the glass, both unaged and aged, was to be utilized in the identification of reactive clusters in the dissolution process. As a first step, the local bonding environment of the network formers (i.e. silicon, boron and aluminum) and the network modifiers (i.e. sodium) was to be characterized by Raman, infrared (IR) and nuclear magnetic resonance (NMR) spectroscopy. In the aged samples these same techniques were to be used in the identification of differential dissolution characteristics as well as the identification of "reactive" species or new species formed during the dissolution process. Using these results a cluster model (Part II) was to be developed allowing the additional identification and ranking of reactive species that are involved in the glass dissolution process. In addition to the above spectroscopic techniques, characterization of the bulk glass and the aged surface by scanning electron microscopy (SEM) was also to be performed.

2. Composition and Characterization of Unaged Glass

Two aluminum borosilicate glass samples were obtained from Johns Manville (batched 3/22/99) in the form of a bulk sample (pre-fiber sample) and 15 μm glass fibers (non-coated). The two samples were characterized, and aged under accelerated conditions. These aged and unaged samples represent the material used for the remainder of investigations described in later sections. The nominal bulk composition as determined by Johns Manville for these glasses is:

SiO_2	54.22 %	MgO	2.77 %
Al_2O_3	13.94 %	SrO	0.01 %
Fe_2O_3	0.23 %	BaO	0.01 %
TiO_2	0.56 %	SO_3	0.01 %
B_2O_3	6.11 %	FeO	0.08 %
Na_2O	1.31 %	Redox	0.37 %
K_2O	0.08 %	Cr_2O_3	106.88 ppm
CaO	20.79 %		

2.1 Differential Thermal Analysis

A TA instrument STD2960 was used for the differential thermal analysis (DTA) allowing the measurement of the glass transition (T_g) onset and the onset of crystallization (T_x) (See Figure 1). DTA samples were prepared by grinding up small piece of each glass (i.e. bulk and fiber) followed by separation through a 150 μm sieve. In all DTA investigations 30-35 mg of sample was utilized, and the analysis performed under argon. DTA were obtained by heating the sample from 25 °C to 1250°C at 10°C/min.

No major differences in T_g and T_x were observed between the unaged bulk and fiber samples.

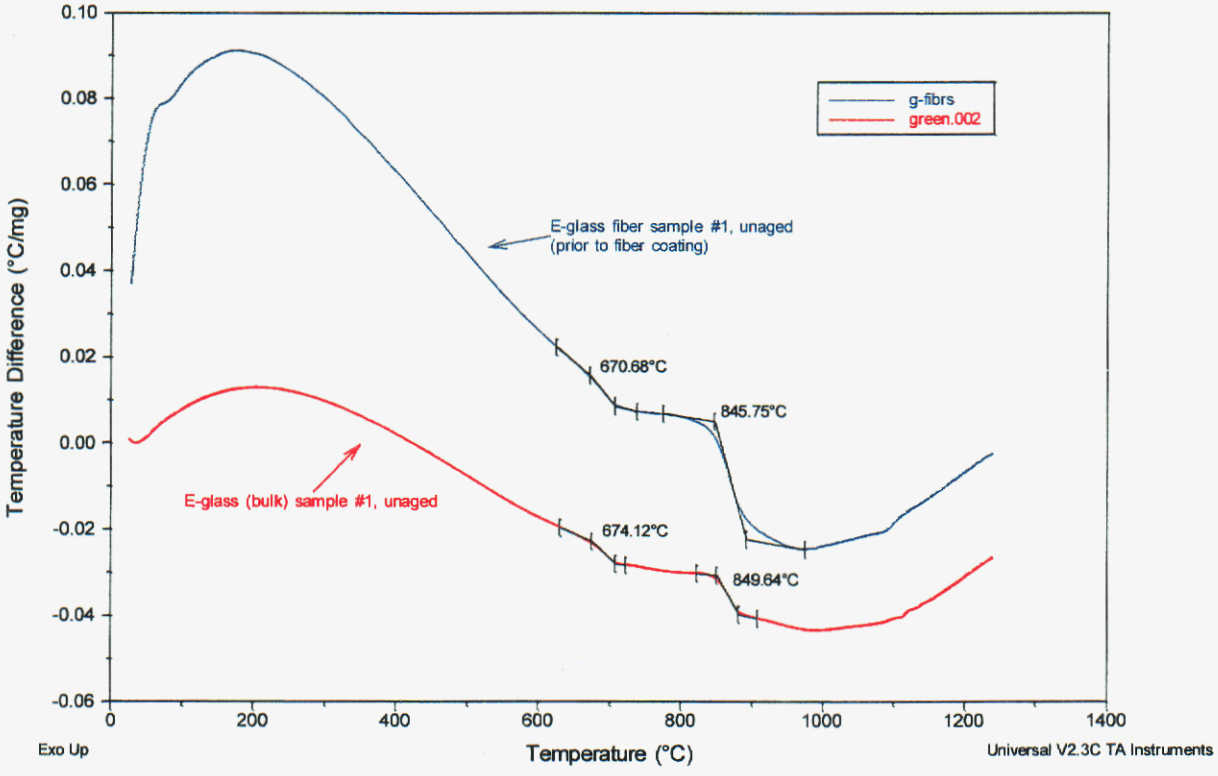

Figure 1: DTA of unaged bulk and fiber JM glass samples.

2.2 Scanning Electron Microscopy Analysis

For the SEM analysis the glass samples were sputter coated with gold/palladium to provide conductivity on the surface of each sample. The cross-sections were obtained by bending the fibers over a scalpel blade and snapping the fibers. (You can see in the images that the fiber cross-sections appear partially cut and partially fractured.) The SEM analysis was performed using 5 KeV accelerating voltage in a Hitachi S4500 Field Emitter Gun SEM. The images and diameter measurements were acquired using PGT (Princeton Gamma-Tech) IMIX digital acquisition software.

The SEM images of the unaged material shows a very clean fracture surface on the bulk glass samples (Figure 2) and a very clean and uniform surface for the glass fibers (Figure 3). The fibers were found to have a relatively uniform diameter of 15 μm, with only a few occlusions observed.

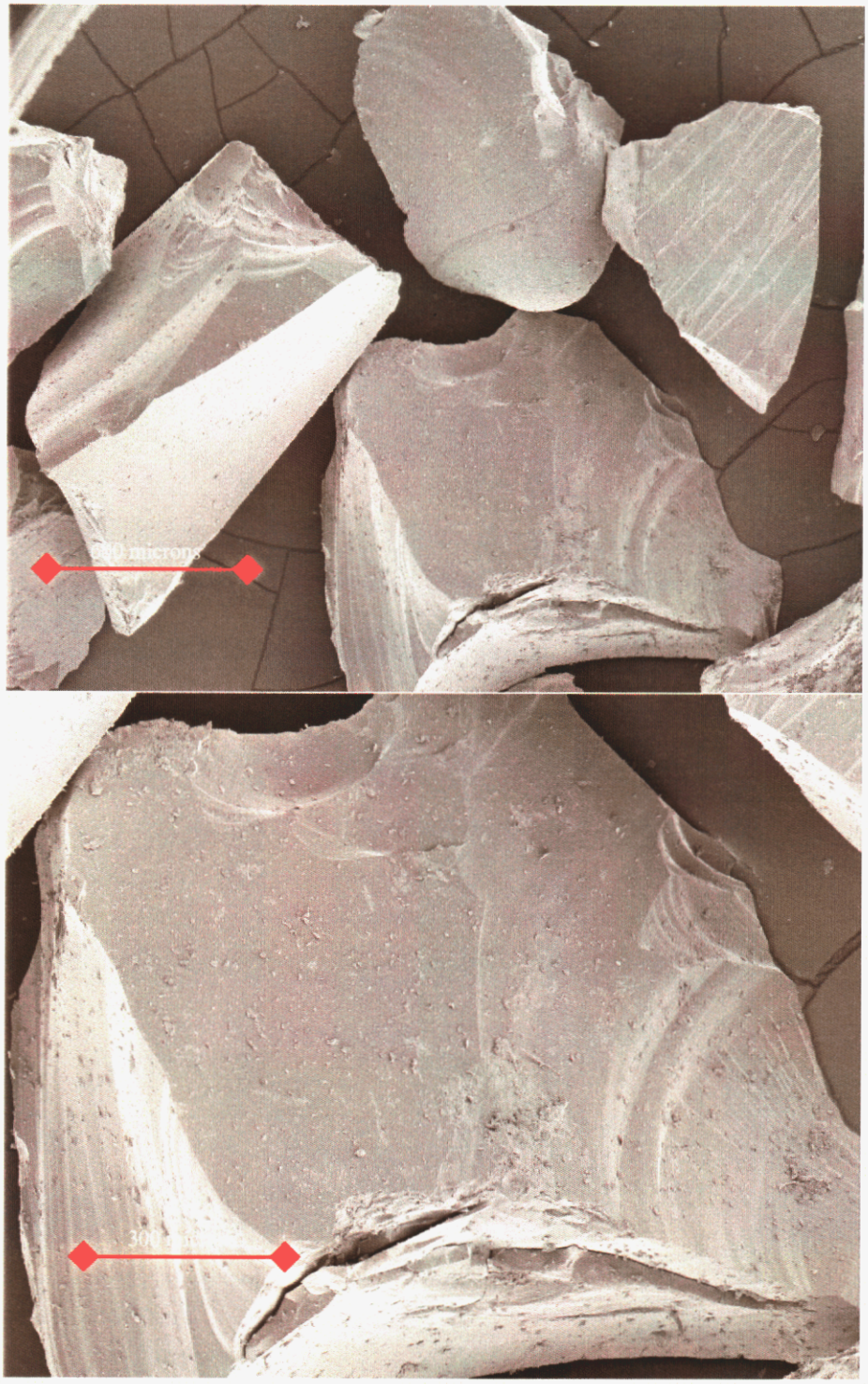

Figure 2: SEM images of unaged bulk glass samples (400 sieve).

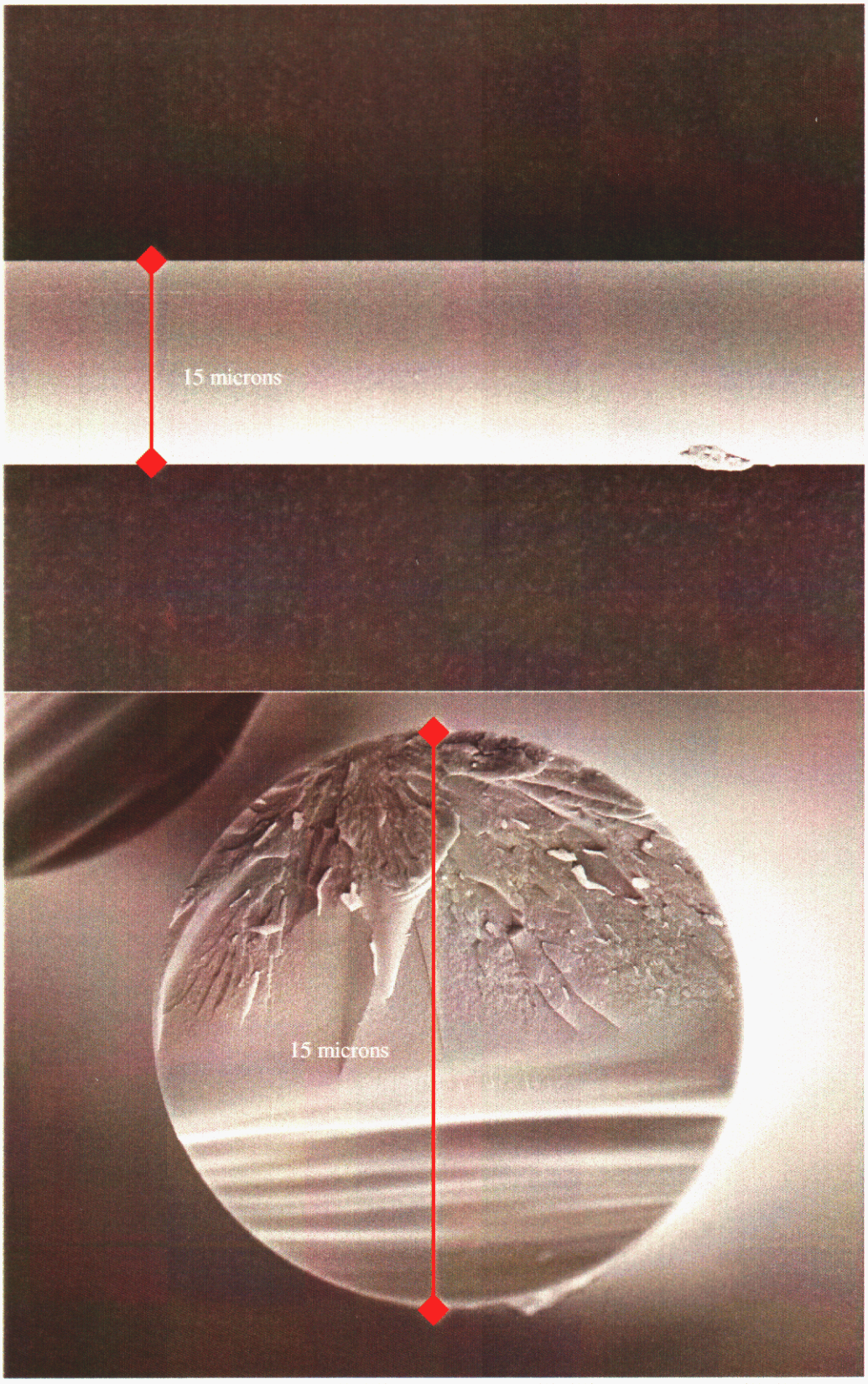

Figure 3: SEM images of unaged fiber.

2.3 Raman Analysis

All bulk and fiber glass samples discussed here are unaged, and were analyzed following cutting and polishing (to 600 grit using SiC) of the bulk sample. Unpolarized, cross and parallel Raman spectra of bulk aluminum borosilicate glass were obtained on 1 cm x 1 cm polished samples using 458 nm excitation. The Raman spectra of the fiber ends, center and on the edge were also obtained for comparison. The 458 nm excitation wavelength is preferred over longer wavelengths because the traces of iron and chromium in the glass fluoresce, and increase the background level at longer wavelengths. Raman spectra of the bulk glass and a fiber glass are shown in Figure 4. Raman spectra of crushed, unaged aluminum borosilicate glass most closely resemble that of the fiber edge (Figure 4). Apparently the presence of ring borates or carbon is associated with the glass surface.

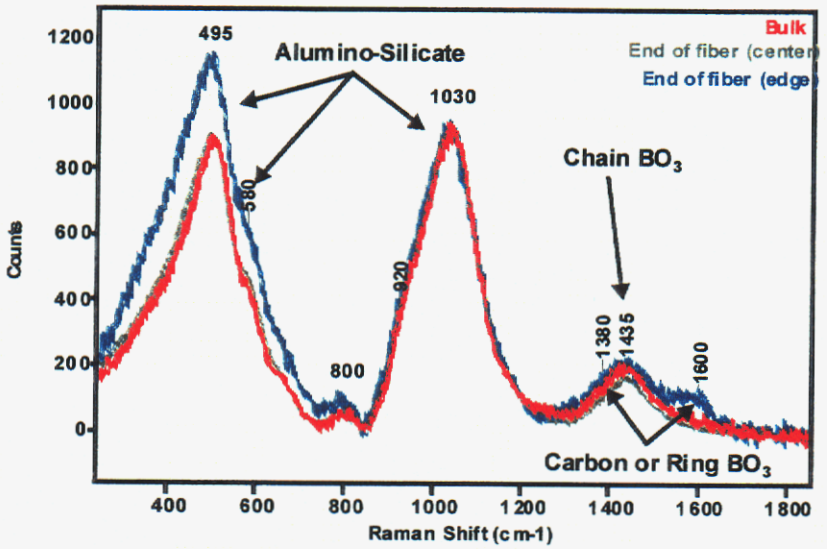

Figure 4: Raman spectra of aluminum borosilicate glass (bulk and fiber).

Our interpretation of the spectra is as follows. The Raman bands occurring below 1100 cm^{-1} are consistent with alumino-silicate glass forms having an Al_2O_3:SiO_2 ratio of approximately 1:3 and sodium/calcium present as modifiers. The lower frequency bands are due to Si-O and Al-O vibrational modes from the aluminosilicate framework. The 495/580 cm^{-1} bands are bending motions (predominantly Si-O-Si), and the 920/1030 cm^{-1} bands are stretching motions of oxygen atoms in silicate tetrahedra modified by networking with aluminum. The weak 800 cm^{-1} band is probably related to Al-O stretching modes, but has also been attributed to various different contributions including the O-Si-O symmetric bond stretch as well as the vibration modes of six-membered rings containing one or two BO_4 groups. The shoulder at 920 cm^{-1} could arise from the B-O-Si stretch or the Q^1 silicon species (where the Q^n nomenclature denotes the number (n) of Si-O-Si bridging bonds). Higher frequency modes are due to chain borate (BO_3) structures in the bulk glass and at the center of the fiber cross-section. The 1380/1435 cm^{-1} bands are due to boron-non-bridging-oxygen stretching motions in chain-type borate polyhedron. Polarization-analyzed spectra are consistent with this interpretation. The bulk glass, the centers of the four fibers analyzed and the edges of two fibers show a high frequency band pattern consisting of the 1380 cm^{-1} shoulder on the 1435 cm^{-1} band. The edges of two fibers, however, have an additional band, peaking near 1600 cm^{-1}, in their spectra (see Figure 4). These features could be due to a thin coating of elemental carbon (typically a carbon-black-like residue of organic material) or a different type of borate structure, composed of rings of borate groups. Metallic cations, such as Ca, Na, etc., present in the structural role of glass network modifiers do not present any Raman bands in the frequency region shown, but their presence affects the positions, shapes and intensities of the bands due to Al-O, B-O and Si-O vibrations. Infrared spectra of unaged, bulk and crushed glass are consistent with our interpretation of the Raman spectra.

2.4 Infrared (IR) Analysis

See section 3.2

2.5 Nuclear Magnetic Resonance (NMR) Analysis

Magic angle spinning (MAS) NMR experiments were performed on ^{11}B, ^{23}Na, ^{27}Al and ^{29}Si nuclei using a 400 MHz Bruker AMX spectrometer modified to include a linear amplifier on the X channel. All experiments were performed using a 4 mm MAS broadband double resonance (HX) probe and a spinning speed of 10 kHz or a 7mm MAS probe spinning at 4 kHz. Additionally, spectra of ^{29}Si were also collected on a Bruker ASX300 using a 7 mm broadband HX probe at 4 kHz MAS. Those spectra collected with the 7 mm probe did not provide any additional information. One-dimensional Bloch decay experiments were performed on all the nuclei. Cross polarization (CP) ^{1}H-^{29}Si experiments were performed using a 5 s recycle delay and a 1 ms contact time. Also, as ^{11}B, ^{23}Na, and ^{27}Al are all quadrupolar nuclei, separation and quantification of their isotropic and quadrupolar components was achieved using the two-dimensional technique known as multiple-quantum (MQ) MAS NMR. This technique requires the creation of triple-quantum coherence and its conversion to single-quantum coherence for observation. Utilizing a z-filter, the MQMAS NMR experiment is made symmetric and the overall coherence pathway becomes $0 \rightarrow \pm 3 \rightarrow 0 \rightarrow -1$. This pathway requires three rf pulses and a minimum of six phase cycles. The first two pulses, $(0 \rightarrow \pm 3 \rightarrow 0)$, are performed using high rf power, ~250 kHz. The third selective pulse is in the power range of ~ 10 – 20 kHz, and brings the evolved MQ magnetization to the single-quantum state for observation. A brief overview of the experimental conditions for each nucleus and experiment is given, below.

2.5.1 ^{29}Si NMR

Silicon experiments of the glass and fibers were collected at 79.5 MHz using a 5 second recycle delay, 1000 signal averages and a $\pi/2$ pulse length of 3.6 us (~70 kHz). Due to the presence of Fe^{2+}, Fe^{3+} and Cr^{3+} in the glass and fibers, spin-lattice relaxation was much quicker than in most silicon based systems. NMR shifts are reported using the δ scale, with positive values being downfield, and are referenced to Q_8M_8, $\delta = 12.2$ ppm.

The direct ^{29}Si NMR spectrum is shown in Figure 5 along with the cross-polarization (CP) $^{1}H/^{29}Si$ experiments. The lack of signal for the CP experiment in the unaged bulk and fiber samples clearly demonstrates that the is no significant proton density in the unaged glass, and that any CP signal observed in the aged sample (see section 3.3.1) results from those species directly produced during the aging process. The broad, slightly asymmetric resonance was deconvoluted according to the procedure previously described by Martin and co-workers.[1-3] The ^{29}Si spectra consists of two Gaussian resonance at δ = -95.2 ppm (FWHM = 1396 Hz) and δ = -85.1 ppm (FWHM = 1147 Hz), corresponding to Q^3 and Q^2 type silicon resonances, respectively (Again the Q^n nomenclature denotes the number (n) of Si-O-Si bridging bonds). Note that there is not any significant pure silica type resonance observed (Q^4 at δ = -110 ppm) in these unaged samples (Figure 6).

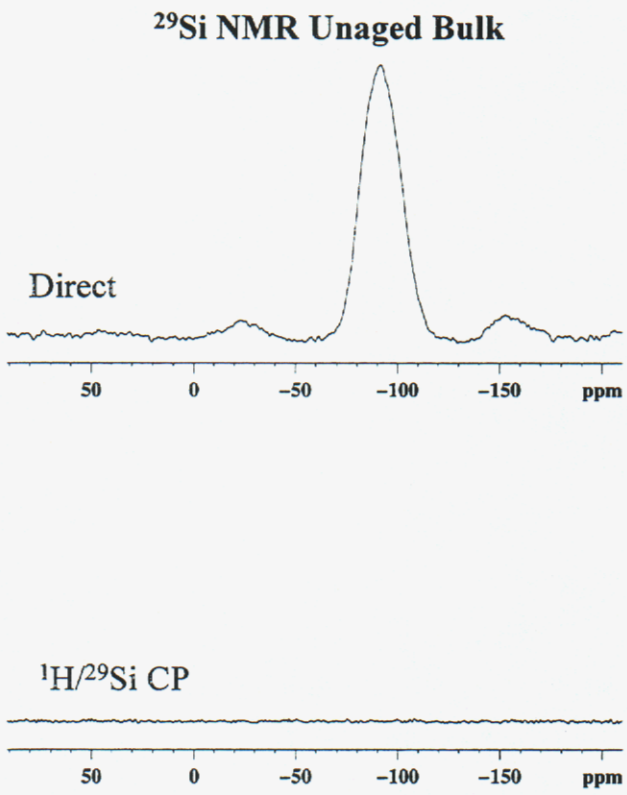

Figure 5: ^{29}Si MAS NMR of unaged bulk aluminum borosilicate glass.

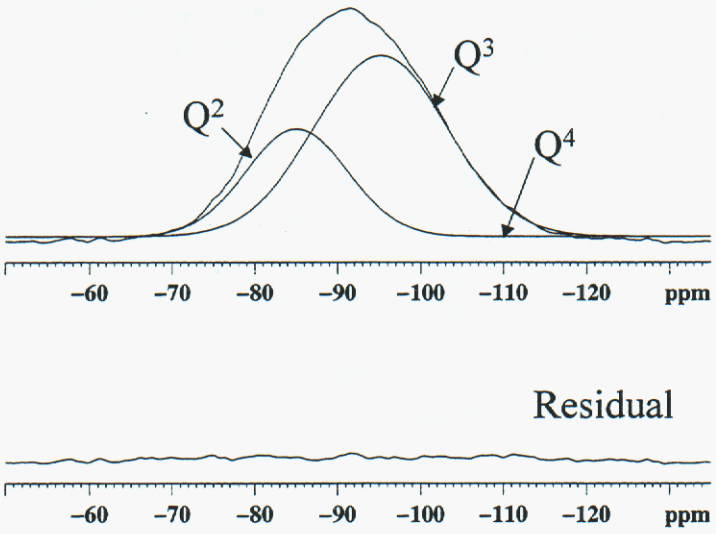

Figure 6: Deconvolution analysis of ^{29}Si MAS NMR - unaged bulk.

2.52 ^{27}Al NMR

Aluminum experiments of the glass and fibers were collected at 104.3 MHz using a 1 s recycle delay, 256 or 1024 signal averages, and a $\pi/2$ pulse of 15 us. In the MQMAS experiment, the length of the two high power rf pulses were 3.3 us and 1.1 us, respectively. The third selective pulse, was set at 15 us (16 kHz). NMR shifts are reported using the δ scale, with positive values being downfield, and are referenced to 1M $Al(H_2O)_6^{3+}$ solution, $\delta = 0.0$ ppm

The ^{27}Al two-dimensional triple-quantum spectra for the unaged CRADA bulk glass is shown in Figure 7. (In the figure ssb refers to spinning side band) The NMR spectrum of the unaged fiber sample is indistinguishable from that of the bulk sample. A single asymmetric resonance is observed, with a center frequency of $\delta = 55$ ppm. No signal arising from the octahedral AlO_6 is observed in the unaged sample. This confirms the hypothesis that the Al is predominantly tetrahedral in nature, and functions as a network former for this glass composition.

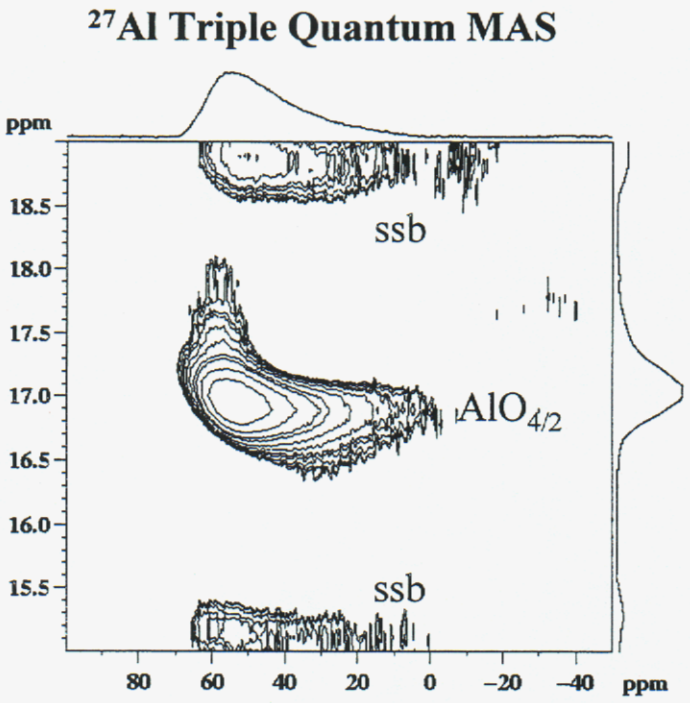

Figure 7: ^{27}Al MQMAS of unaged bulk aluminum borosilicate glass.

2.5.3 ^{23}Na NMR

Sodium experiments of the glass and fibers were collected at 105.85 MHz using a 1 s recycle delay, 128 signal averages, and a $\pi/2$ pulse of 15 us. In the MQMAS experiments the length of the two high power rf pulses were 4.4 us and 1.4 us, respectively. The third selective pulse, was set at 15 us (16 kHz). NMR shifts are reported using the δ scale, with positive values being downfield, and are referenced to 1M NaCl solution, $\delta = 0.0$ ppm

Only one resonance is visible in the ^{23}Na spectrum (Figure 8) at –19.2 ppm (FWHM = 2100 Hz) in the unaged glass. Koller et al. [4] presented a relationship between the ^{23}Na chemical shift and the chemical shift parameter A given by

$$\delta_{cs} = -133.6A + 107.6 \qquad (1)$$

where the parameter A involves the valence of the coordinating oxygen (W), the average Na-O distance ($r_{Na\text{-}O}$) and the coordination number CN of the sodium. The parameter A is defined by

$$A = CN\langle W\rangle / \langle r_{Na\text{-}O}\rangle^3 \qquad (2)$$

Assuming an average oxygen valence of $W \sim 2$, and a Na-O bond length of ~ 2 Å, the observed chemical shift in consistent with Na atoms having a coordination number CN ~ 4.

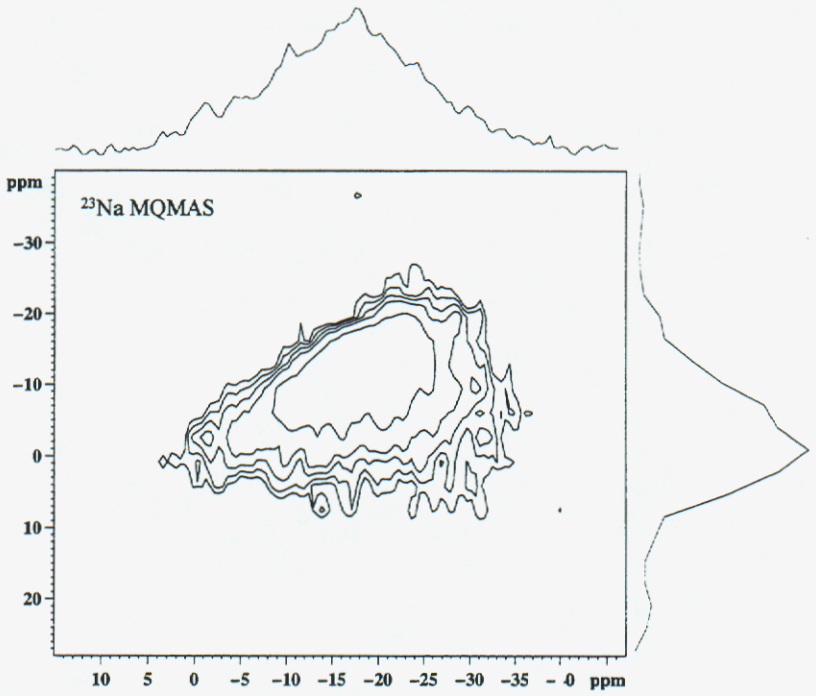

Figure 8: ^{23}Na MQMAS of unaged bulk aluminum borosilicate glass.

2.5.4 ^{11}B NMR

Boron NMR experiments of the glass and fibers were collected at 128.4 MHz using a 5 s recycle delay, 64 signal averages, and a variety of $\pi/2$ pulse lengths: 52 us, 30 us, 15 s and 0.9 us. Due to the presence of boron in the probe's background, a two pulse "depth" phase cycled program was used to minimize its effect on the acquired spectra. NMR shifts are reported using the δ scale, with positive values being downfield, and are referenced to 1M $BF_3{\cdot}(OEt_2)$, $\delta = 0.0$ ppm. The MQMAS experiment allows for separation and quantification of the boron sites. The length of the two high power rf pulses were 3.5 us and 1.2 us. The third selective pulse was set at 30 us (8 kHz). A 5 second recycle time was used.

The ^{11}B MAS NMR one-dimensional spectra (Figure 9) and the two-dimensional triple-quantum MAS spectra (Figure 10) for the unaged glass samples are shown below. From these NMR results the triganol BO_3 and the tetrahedral BO_4 sites are clearly resolved. Simulations of the relative concentrations demonstrate that BO_3 is the dominate boron species (~90%), while the remainder of the boron is present as BO_4 (~10%) (Figure 9). The BO_3 species show significant second order quadrupolar broadening allowing an estimation of the quadrupolar coupling constant, QCC ($= e^2qQ/h$) and asymmetry parameter η_Q. For the unaged CRADA glass samples these quadrupolar parameters were found to be QCC = 2.69 MHz and $\eta_Q = 0.35$. The increase in the asymmetry parameter suggest that the D_{3h} symmetry has been disrupted for the three coordinate boron. This decrease in symmetry demonstrates that the trigonal borons are most likely assigned to distorted BO_2O^- species.[5] In Figure 10 the dispersion (or stretch) of the individual resonances in the isotropic dimension (vertical) clearly demonstrates that there is significant chemical shift dispersion for these species, reflecting variation in the local bonding geometry.

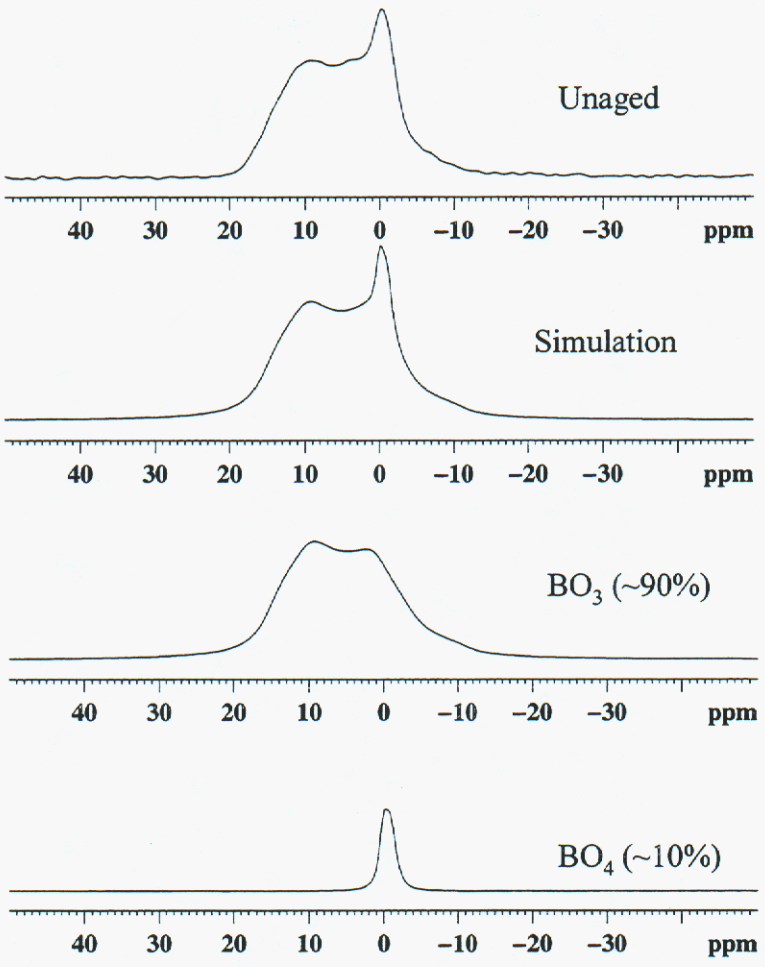

Figure 9: ^{11}B MAS NMR of unaged bulk aluminum borosilicate glass.

^{11}B Triple-Quantum Magic Angle Spinning NMR

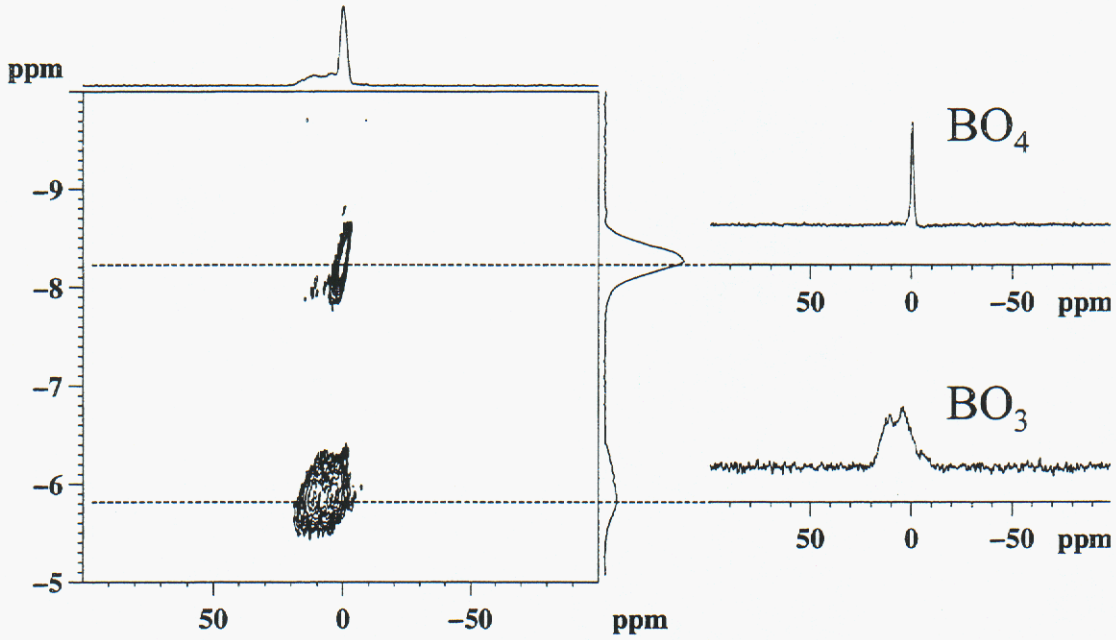

Figure 10: ^{11}B MQMAS of unaged bulk aluminum borosilicate glass.

3. Characterization of Aged Aluminum Borosilicate Glass Samples

Prior to aging of the bulk CRADA glass, samples were crushed and sieved into four (4) different sizes. Mesh sizes are commonly referred to in the description of the sample. These are:

Mesh	Opening (in.)	Opening (um)
400	0.0015	38
100	0.0059	149
60	0.0098	250
35	0.0197	500

The glass fibers were aged as received without further modification. Three different aging protocols were employed; 1) acidic aqueous conditions (representing a very corrosive environment) 2) neutral aqueous conditions, and 3) very basic conditions.

Acidic Conditions

Crushed CRADA glass (400 mesh), fibers and cut-cubes were placed in 1N HCl and kept at room temperature. At 90 hours, a sample of the 400 mesh glass was obtained and analyzed by $^{1}H/^{29}Si$ CP NMR for possible aging effects. Spectra for this acid aged sample were obtained and are discussed below. Samples of bulk glass and glass fibers aged for 200 to 250 hours at room temperature have been obtained, and were analyzed by SEM.

Neutral Conditions

The CRADA crushed glass, fibers and cut-cubes were kept immersed in 95°C de-ionized water. Samples were aged up to 236 days under these conditions. The dissolution rate in these solutions was very small, and was measured as 1.6×10^{-9} g/min cm^2 averaged over 236 days.

Base Conditions

Crushed CRADA glass (400 mesh), fibers and cut-cubes were placed in 1N NaOH and allowed to react at room temperature. Samples aged up to 18 days were obtained, and analyzed with NMR to address possible aging effects. Spectra for these aged samples are discussed below.

3.1 SEM Analysis

Aged bulk and fiber samples were prepared and analyzed as described in the unaged section 2.2. Inspection of the SEM images for the acid aged bulk glass samples show a highly cracked and defoliated surface, resulting from the drying of the hydrated "aged" surface (Figure 11). The images of the fibers aged under acid conditions (Figure 12) reveal that the over all diameter of the fibers has been reduced from the initial 15 μm to diameters ranging from 12-14 μm. In addition, very uniformly spaced stress cracks are observed to form in these aged fiber samples. Calculation of the original stress in these aged surfaces should be possible, but where not pursued in this case.

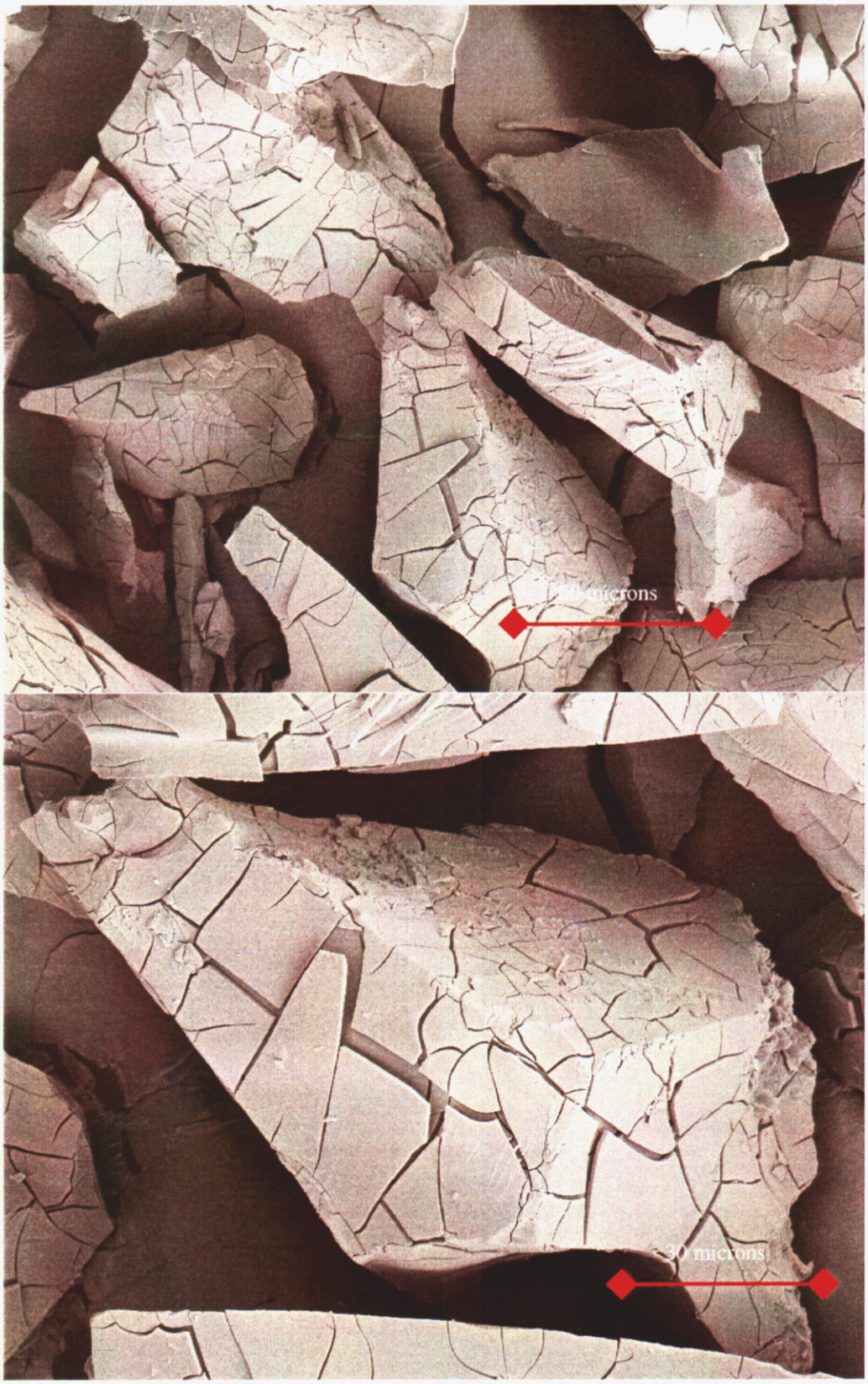

Figure 11: SEM of acid aged bulk aluminum borosilicate glass.

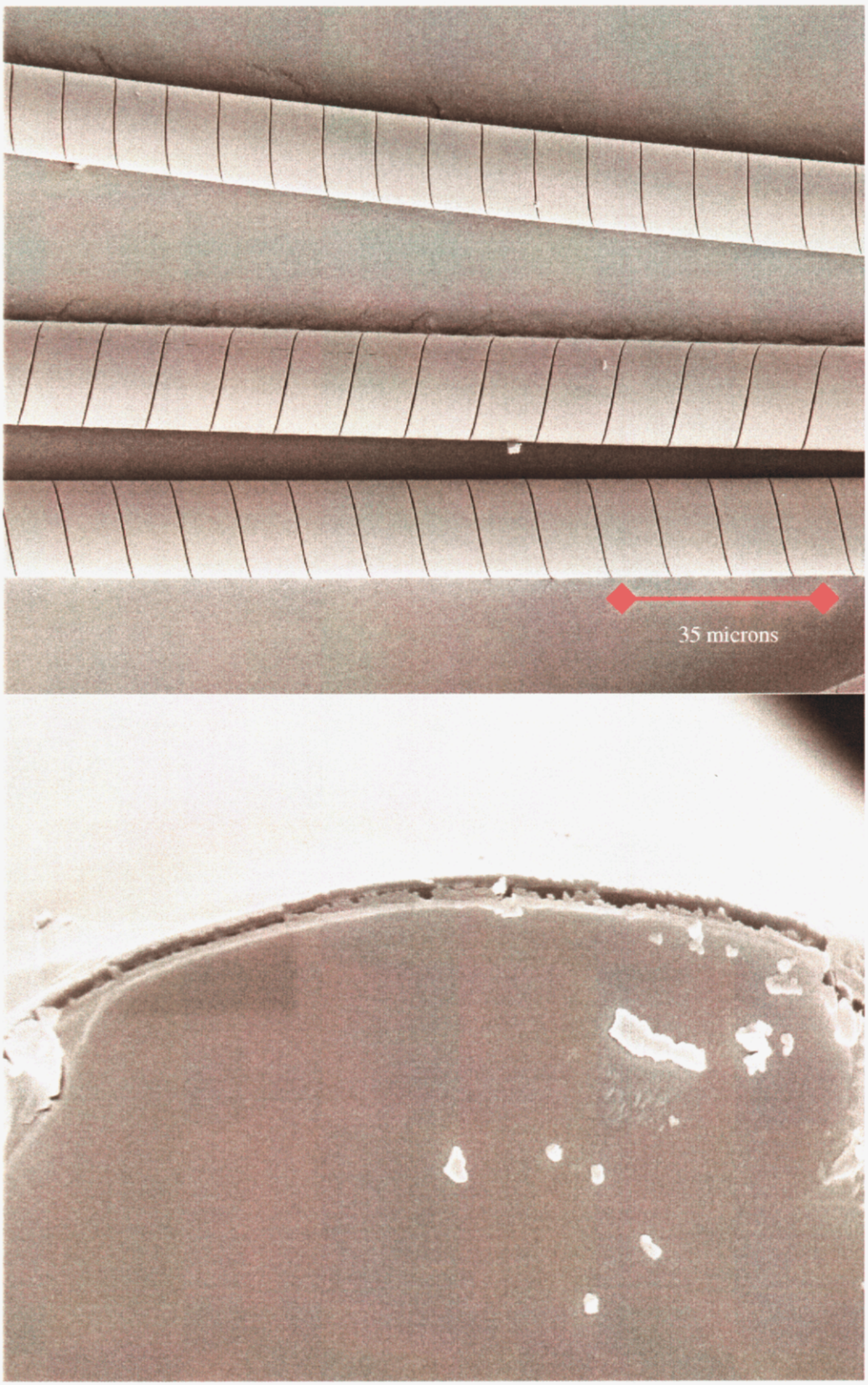

Figure 12: SEM of acid aged aluminum borosilicate glass fibers.

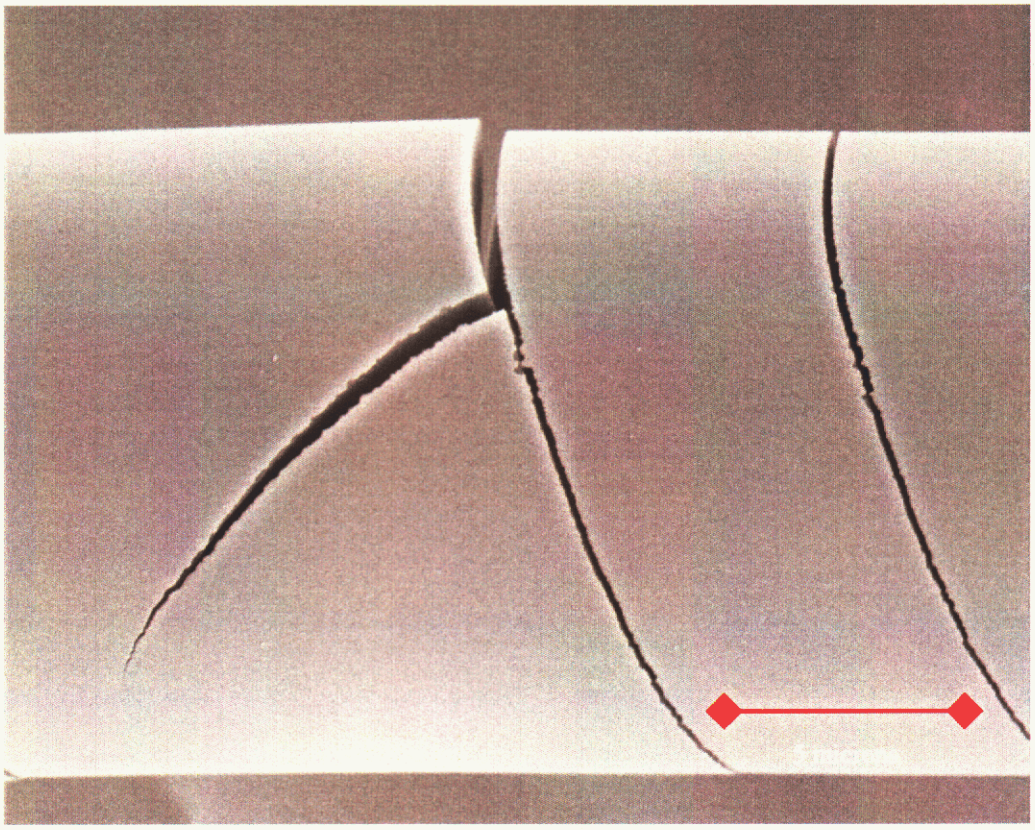

Figure 13: SEM image of stress cracks in aged aluminum borosilicate glass fibers.

3.2 Raman and IR Analysis

Raman spectra of the crushed aluminum borosilicate glass (Figure 14) after aging in 1 N HCl show significant changes, which can be associated with leaching. The bands due to the alumino-silicate framework have been replaced with bands associated with hydroxylated silica, implying leaching of aluminum and the metallic cations (Ca, Na, etc.) present as network modifiers in the unaged glass. The remaining framework is a porous, silanol-terminated, silica network with a mixture of chain and ring borate structures.

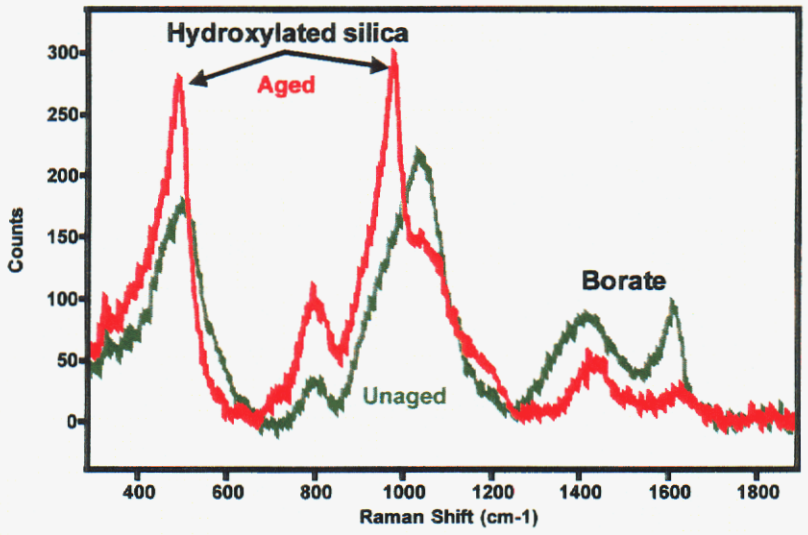

Figure 14. Raman spectra of bulk aluminum borosilicate glass (aged and unaged).

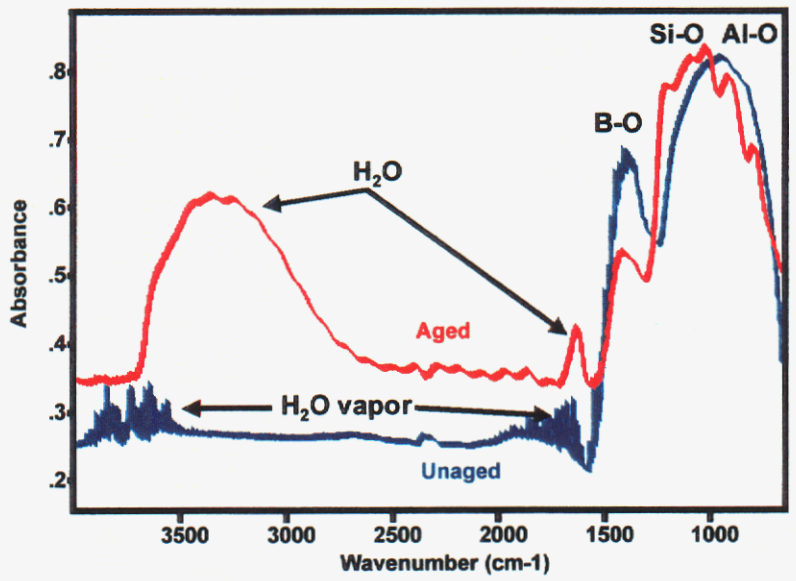

Figure 15. Infrared transmission spectra of (aged and unaged) bulk aluminum borosilicate glass.

Infrared spectra of aged, crushed bulk aluminum borosilicate glass (Figure 15) indicate a similar picture of leaching: a change from an aluminosilicate to a silicate framework and differences in the borate structures. In addition the infrared spectra show the presence of a large amount of adsorbed water, consistent with a porous silica framework, in the crushed, aged glass, whereas little or no water was present before aging.

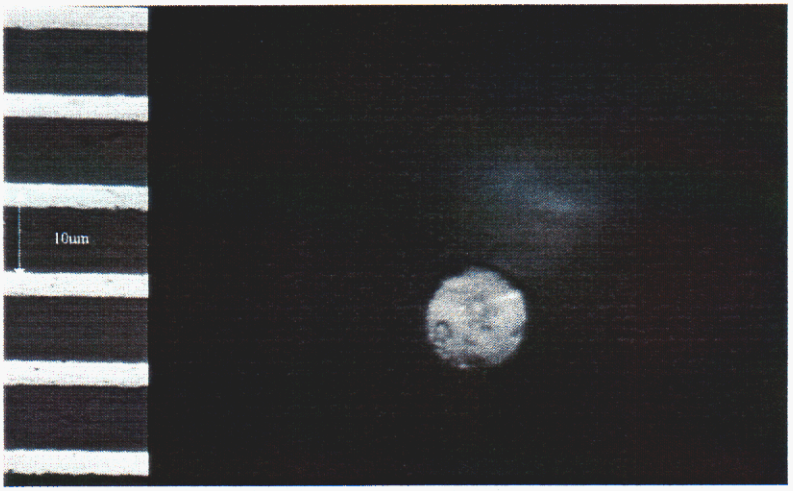

Figure 16. Micrograph of unaged fiber end.

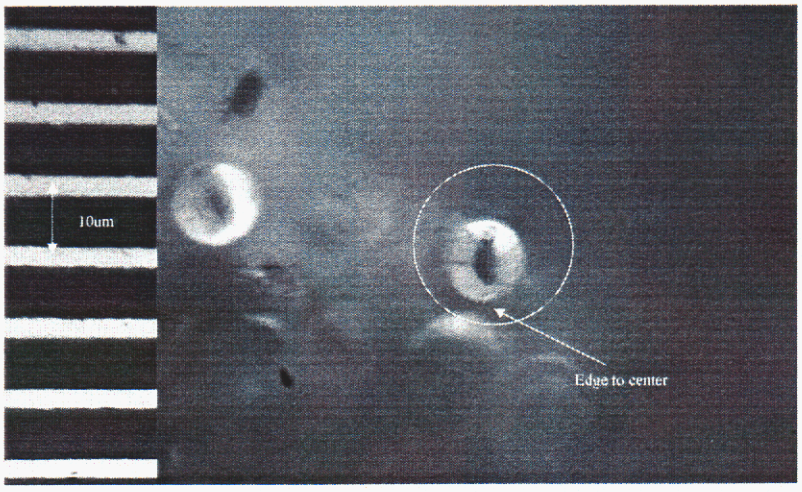

Figure 17. Micrograph of aged fiber end.

Figures 16 and 17 show optical micrographs of the ends (cross-sections) of aged (1 N HCl) and unaged glass fibers. The unaged fibers and the centers of most aged fibers look transparent (the centers of the aged fibers appear darker in the optical micrographs because of differences in their exposures and contrast). The outer portions of the aged fibers are opaque. Using our micro-Raman capability, which has a horizontal spatial resolution of a micrometer and samples several micrometers in depth, we obtained Raman spectra across the cross-section of the fiber circled in Figure 17. These Raman spectra are shown in Figures 18 and 19.

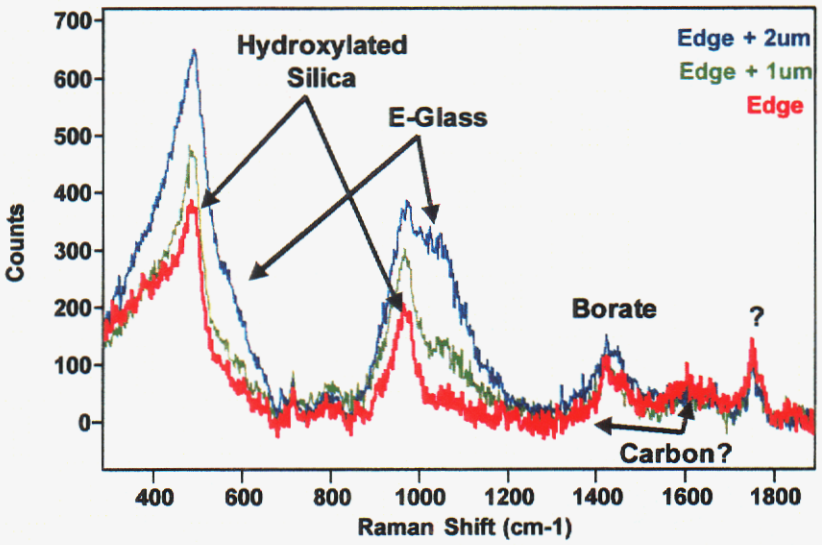

Figure 18. Micro-Raman spectra of outer locations on the end of aged fiber.

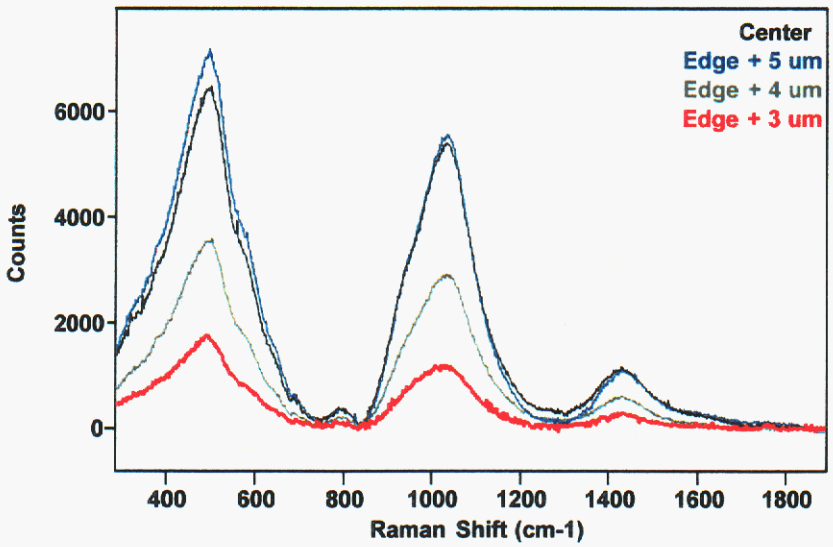

Figure 19. Micro-Raman spectra of inner locations on the end of the aged fiber (same fiber as Figure 18).

The Raman spectrum from the edge of the fiber cross-section is much like that from the aged, crushed glass (Figure 14). At the edge of the fiber, the glass framework is hydroxylated silica, and either ring borate or carbon structures have been added to the borate chains initially present. In fact the borate bands have narrowed, suggesting crystallization from the original glass framework. In addition, the spectrum from the edge of the fiber (Figure 18) has a band peaking near 1800 cm^{-1} (marked with a "?"). The most likely source for this band is a carbonyl (probably carboxylate) group, but it is not clear how a carboxylate-containing material was deposited on the glass fiber. Similar bands, peaking near 1800 cm^{-1}, are present in the spectra of other aged fibers.

The Raman spectra indicate that the edge of this fiber is highly leached. The leached region extends two to three micrometers into the fiber cross-section, at which point the Raman spectra begin to show the presence of unleached glass (Figure 18). By the center of the cross-section of the aged fiber (Figure 19), the Raman spectra are that of glass with no apparent leaching. Other fibers, however, show evidence of leaching (silica bands and modified, crystallized borate structures) through to the center of the fiber (Figure 20), suggesting some differential dissolution behavior between fibers.

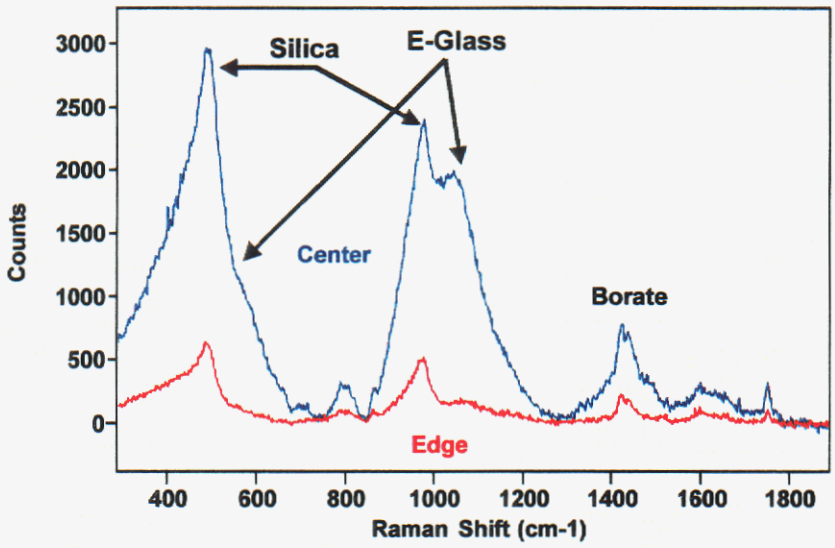

Figure 20. Micro-Raman spectra of inner locations on the end of another aged fiber, which appears to be partially leached at its center

The vibrational spectra of bulk, unaged aluminum borosilicate glass indicate that it has the expected structure, with an aluminosilicate framework and chain BO_3 structures. The structure of unaged glass fibers is the same, except for some differences in the borate structures at edge of the borate fiber cross-section. Crushed, unaged aluminum borosilicate glass also has the same framework but some differences from bulk glass in its borate structures. Aging in 1N HCl results in leaching that removes aluminum and network modifier cations (Na^+, Ca^{++}, etc.) and that rearranges and tends to crystallize borate structures, possibly removing some from the glass network. The resulting, leached glass framework is composed largely of hydroxylated silica. The leaching effect is more obvious in the Raman spectra of the aged, crushed glass samples than in the spectra of the bulk, aged samples. The leached layers tend to flake off the bulk glass, but the remaining leached glass matrix was detected using infrared reflection techniques. The aged fibers show an outer leached layer, generally extending a few micrometers towards the center of the fiber cross-section. Some fibers show evidence of leaching to the center of their cross-section.

3.3 NMR Analysis

3.3.1 ^{29}Si NMR

The ^{29}Si NMR spectra for the bulk sample aged under acid conditions is shown in Figure 21. Several important observations can be made. First, the CP spectra now shows three distinct resonances (compared to no signal for the unaged sample). These resonances are distinct from the bulk signal, and arise only from those silicon environments in the hydrated "aged" layer. Following spectral deconvolution (Figure 22) the upfield resonance at δ = -109 ppm can be assigned to Q^4 pure silica type resonance, (SiO_4), while the dominant resonance at δ = -100 ppm results from the SiO_3OH type species, and the δ = -91 ppm arising from a Q^2 type species. From these spectra it is clear that the silicon environment in the surface layer is significantly different than the bulk glass, and that silicon rich species are observed to remain in the aged surface, and result from the condensation of hydroxylated silicon produced during dissolution.

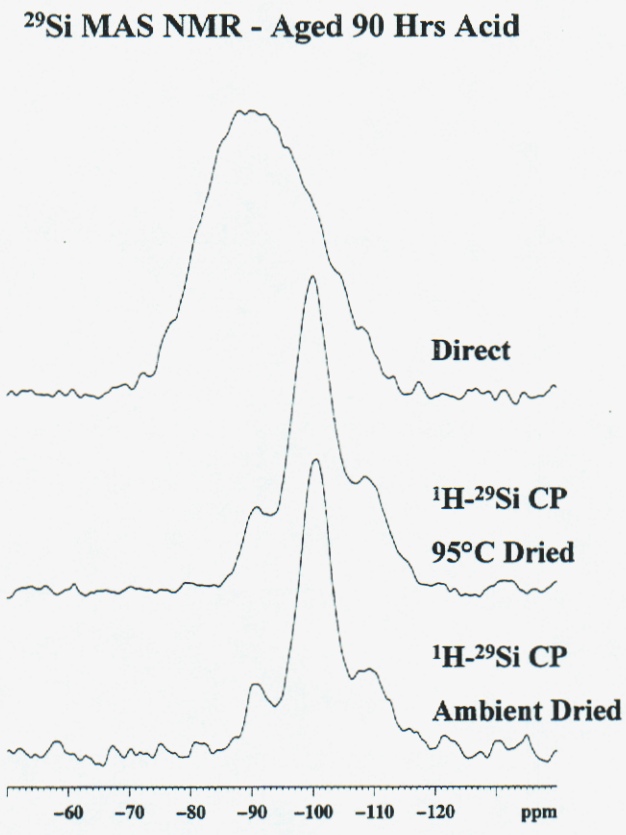

Figure 21: ^{29}Si MAS NMR of acid aged bulk aluminum borosilicate glass.

^{29}Si CP MAS - Acid Aged Bulk

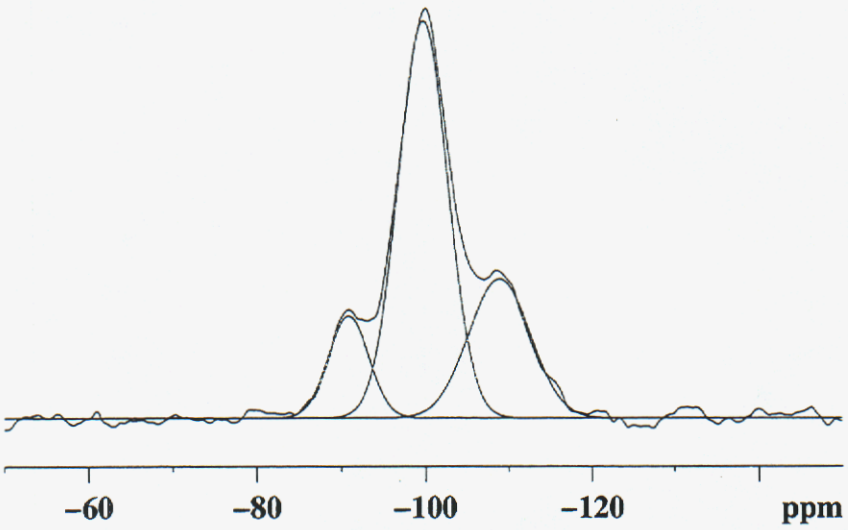

Figure 22: Deconvolution of ^{29}Si NMR spectra of acid aged aluminum borosilicate glass.

Similar ^{1}H-^{29}Si CP MAS NMR experiments were also performed on bulk glass samples aged under neutral and basic conditions. These spectra are shown in Figure 23. The CP signal for these samples is significantly weaker than that observed in the acid aged glass, consistent with the lack of a significant hydrated gel layer being formed under these conditions. In the aged surface of the base material there is a preferential formation of Q^1 and Q^2 species in comparison to the unaged distribution. Even though the aged surface contributes a small signal, it is clear that new silicon containing species are being formed. This observation contrast to the ^{1}H-^{29}Si CP MAS spectra observed for the glass aged under neutral conditions, in which the Q^n distribution is very similar to that observed for

the unaged glass sample. The lack of a significant hydrated gel layer (and corresponding low CP signal) in the neutral and acid aged samples, would make future multinuclear correlation experiments as well as more detailed investigations of Si-Si connectivities difficult. No differences were observed in the direct spectra between unaged and aged glasses.

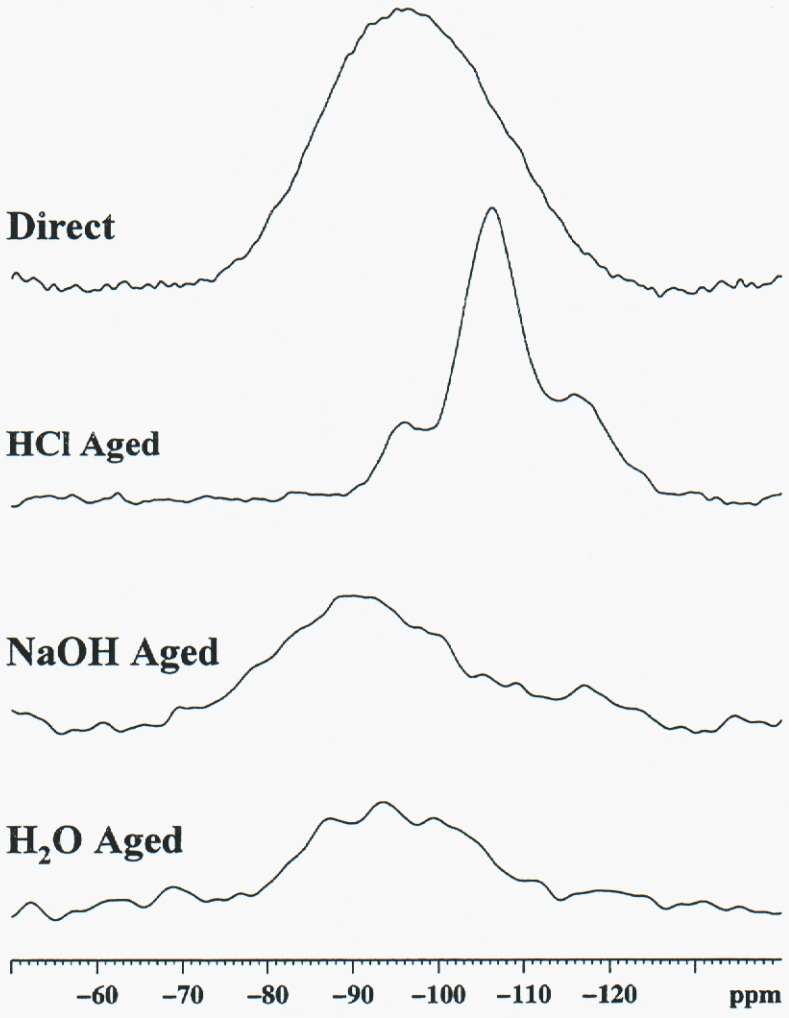

Figure 23: ^{29}Si CPMAS NMR spectra of aged aluminum borosilicate glass.

3.3.2 ^{27}Al NMR

The ^{1}H-^{27}Al CP MAS spectra for the acid aged glass is shown in Figure 24. The CP signal is very weak, suggesting that Al is not a major constituent of the hydrated surface produced in the acid aged glass. The sharp resonance observed corresponds to a tetrahedral (IV) Al species, with no indication of (V) and (VI) coordinated Al being present in the hydrated surface. No differences were observed in comparison of the unaged and acid aged direct ^{27}Al NMR spectra (not shown).

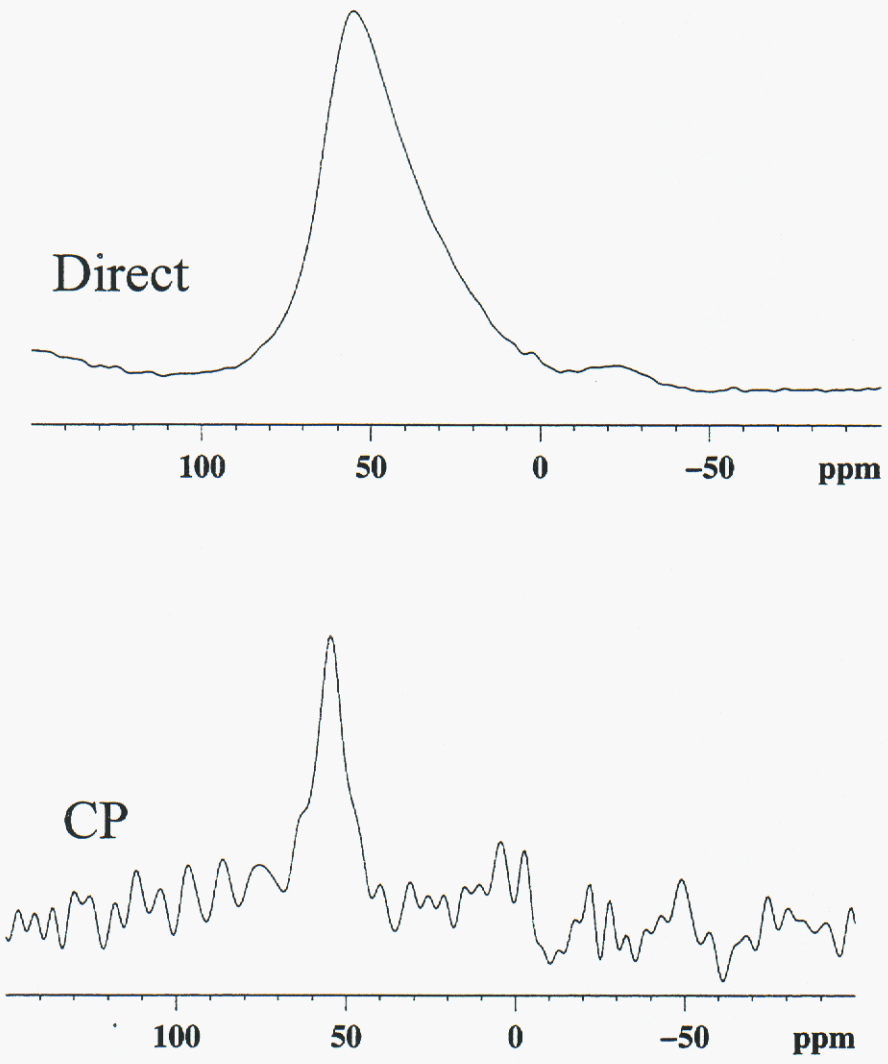

Figure 24: ^{27}Al CPMAS NMR spectra of acid aged aluminum borosilicate glass.

3.3.3 ^{11}B NMR

Figure 25 shows the direct Block decay spectra and the ^{1}H-^{11}B CP MAS spectra for acid aged aluminum borosilicate glass. The CP signal is *extremely* weak and very broad, demonstrating that there is not significant boron remaining within the hydrated surface layer. No differences between the unaged and aged glasses was observed for the direct ^{11}B NMR spectra (not shown).

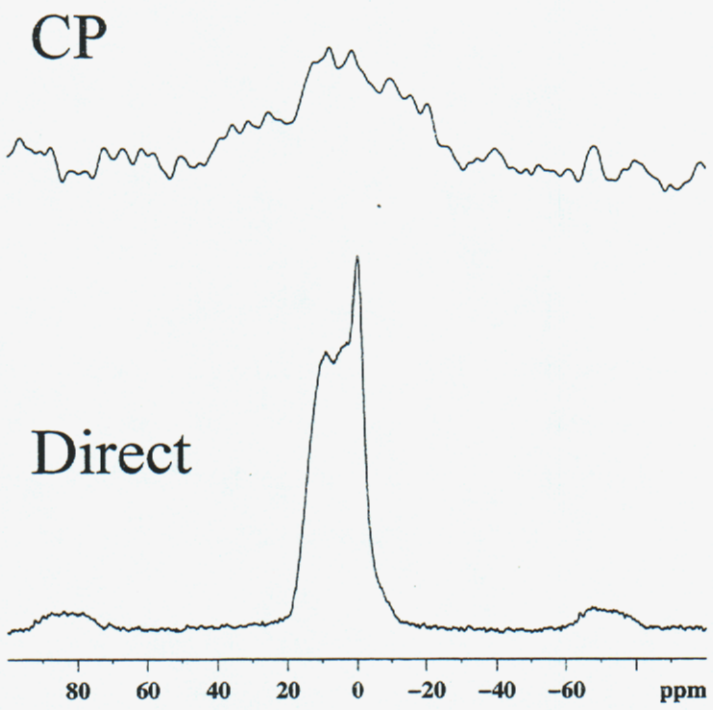

Figure 25: ^{11}B CPMAS NMR spectra of acid aged aluminum borosilicate glass.

4. Discussion

The corrosion of dissolution of glasses can in general be described by the equations

$$(RO)_3Si\text{-}O\text{-}M+H_2O \longrightarrow (RO)_3Si\text{-}OH+MOH$$

$$(RO)_3B\text{-}O\text{-}M+H_2O \longrightarrow (RO)_3B\text{-}OH+MOH \qquad (3)$$

$$(RO)_2B\text{-}O\text{-}M+H_2O \longrightarrow (RO)_2B\text{-}OH+MOH$$

where RO represents the remaining oxide bonds to the surrounding glass structure. The calculation of the reaction enthalpies for this class of dissolution and ion exchange reactions will be discussed in Part II. The spectroscopic analysis of these glasses was able to describe the local structure of these network formers and select modifiers in the unaged aluminum borosilicate glass. In particular there was a broad distribution of Q^n species for Silicon, both 3- and 4-coordinate Boron, predominantly tetrahedral (IV) Aluminum, with the Na modifier showing an average coordination number of four. The NMR analysis was not able to see any significant differences between fiber and bulk, while the Raman analysis clearly show a difference of local structure at the very edge or surface of the glass fibers.

These techniques were able to characterize new species formed in the aged surface. The NMR and Raman results clearly demonstrate that a hydroxyl-rich silicon layer is formed during the acid corrosion of the aluminoborosilicate glass, (through the eqns. 3). In addition the NMR results demonstrate that a condensation reaction involving the silanols produced is also occurring within the gel layer, and can be described by

$$2[(RO)_3\text{-}Si\text{-}OH] \longrightarrow (RO)_3\text{-}Si\text{-}O\text{-}Si\text{-}(OR)_3+H_2O \qquad (4)$$

Observation of a similar condensation type reactions using ^{29}Si MAS NMR has also been reported for a potash-lime-silicate glass.[6] The microscopic Raman analysis clearly show

that a significant hydrated gel like layer is formed on aged fibers under acid conditions, and that the leaching of boron is graduated across this surface. The lack of CP NMR signal for the ^{27}Al and ^{11}B species also supports the almost complete leaching of these species from the hydrated surface.

While significant details were obtained for the local structure in the unaged glass using these spectroscopic techniques, the lack of observable differential species dissolution, as well as limited number of new species identified in the aged surface, makes the input for the computational studies rather limited. Any further endeavors into the identification of reactive species at the dissolution surface will need to address this inability to observe differential reactivity.

5. References

1. Bhasin, G., Bhatnagar, A., Bhowmik, S., Stehle, C., Affatigato, M., Feller, S., MacKenzie, J. and Martin, S. *Phys. Chem. Glasses* **39**, 269-274 (1998).

2. MacKenzie, J. W., Bhatnagar, A., Bain, D., Bhowmik, S., Parameswar, C., Budhwani, K., Feller, S. A., Royle, M. L. and Martin, S. W. *J. Non-Cryst. Solids* **177**, 269-276 (1994).

3. Marin, S. W., Mackenzie, J. W., Bhatnagar, A., Bhowmik, S., Feller, S. A. and Royle, M. L. *Phys. Chem. Glasses* **36**, 82-88 (1995).

4. Koller, H., Englehardt, G., Kentgens, A. P. M. and Sauer, J. *J. Phys. Chem.* **98**, 1544-1551 (1994).

5. Züchner, L., Chan, J. C. C., Müller-Warmuth, W. and Eckert, H. *J. Phys. Chem. B* **102**, 4495-4506 (1998).

6. Böhm, T.; Leissner, J. *Glastech. Ber. Glass Sci. Technol.* **68**, 400-403 (1995).

Distribution:

15	Dr. Diana Fisler, Johns Manville 10100 West Ute Avenue Littleton, CO 80127	
15	MS 1407	T. Alam
1	MS 1407	D. Lang
1	MS 1349	D. Bencoe
1	MS 1411	D. Tallant
1	MS 1411	R. Simpson
1	MS 1405	B. McKenzie
1	MS 1411	M. Garcia
1	MS 9018	Central Technical Files, 8940-2
2	MS 0899	Technical Library, 9616
1	MS 0612	Review & Approval Desk, 4912 For DOE/OSTI
1	MS 1380	Technology Transfer, 4331